A modified multi-site occupancy model: evaluation of azeotropelike behavior in adsorption

L. L. Romanielo · S. Arvelos · F. W. Tavares · K. Rajagopal

Abstract Even though a large number of statistical-mechanics models can be found in the literature to describe adsorption, no one is good enough to reliably predict some highly non-ideal behavior, such as the inversion of selectivity presented in the adsorption of some mixtures. This is probably due to the natural complexity of adsorption phenomena, which can be attributed to several factors such as the non-uniformity of the solids and the intermolecular forces between adsorbent-adsorbate and adsorbate–adsorbate. In order to contribute to the improvement of the models, this paper presents a study of the impact of the relative molecule sizes and the lateral interactions for the azeotropelike behavior in adsorption. Therefore, we present here a modified model based on the Nitta et al. (1984) Multi-Site Occupancy Model (MSOM). The ability of the model proposed here to describe binary and ternary adsorption mixtures was compared to the one obtained from the original Nitta et al. (1984) model and by the Vacancy Solution Model (VSM, from Suwanayuen and Danner 1980a, b). The results showed that the relative size of the molecules and the lateral (adsorbate–adsorbate) interactions are very important variables in the description of the azeotropelike behavior. Even though the MSOM requires fewer parameters obtained from pure isotherm data, compared to VSM, it presented better performance for both binary and ternary mixtures. The proposed MSOM was able to predict the majority of the azeotropelike behavior studied here.

Keywords Adsorption · Azeotropelike behavior · MSOM · VSM

1 Introduction

A reliable description of adsorption of mixtures on solid surfaces or inside solid structures, such as confined fluids, is very important in order to optimize numerous industrial processes. In practice, adsorption processing involves multicomponent mixtures, which can exhibit highly non-ideal behavior.

According to Dunne and Myers (1994), the causes of non-ideality are related to differences in polarity, molecular size and shape, in addition to the energetic heterogeneity of the adsorbents. Here, we are going to focus on adsorption on energetic-homogeneous surfaces. We show that even for homogeneous surfaces, the adsorption can present highly non-ideal behavior due to molecular size and shape and the interaction between molecules adsorbed in neighboring sites. In the literature, there are systems that present azeotropelike behavior in which there is an inversion in adsorption selectivity. These systems are quite useful for evaluating the performance of adsorption equilibrium models.

We present here a modified version of the multi-site occupancy model (MSOM-M) proposed originally by Nitta

L. L. Romanielo (✉) · S. Arvelos
Faculdade de Engenharia Química, Universidade Federal de Uberlândia, Av. João Naves de Ávila, 2121,
CEP 38408-144 Uberlândia, MG, Brazil
e-mail: lucienne@ufu.br

F. W. Tavares
Programa de Engenharia Química, COPPE, Universidade Federal do Rio de Janeiro, Cidade Universitária, CP 68502,
CEP 21941-972 Rio De Janeiro, RJ, Brazil

F. W. Tavares · K. Rajagopal
Departamento de Engenharia Química, Escola de Química, Universidade Federal do Rio de Janeiro, Cidade Universitária,
CEP 21949-900 Rio De Janeiro, RJ, Brazil

et al. (1984). The performance of the proposed model (MSOM-M) was evaluated in terms of the prediction of binary and ternary adsorption mixtures. The model performance was compared to the one presented by the original MSOM and to the vacancy solution model (VSM) presented by Suwanayuen and Danner (1980a, 1980b).

2 Adsorption isotherm models

The canonical ensemble partition function, representing the adsorption of a single component, expressed in terms of the number of molecules (N), number of sites (M) and temperature (T), is given by:

$$Q(N, M, T) = q(T)^N g(N, M) \exp\left(\frac{\bar{E}_c}{kT}\right) \tag{1}$$

where $q(T)$ is the internal partition function of a molecule, $\bar{E}_c$ is the average configurational energy, and $g(N,M)$ is the number of configurational states.

The statistical thermodynamics hypotheses for Langmuir isotherm are: (a) a fixed number of vacant or adsorption sites are available on the surface; (b) all the vacant sites are of equal size, shape and energy on the surface; (c) each site can hold the maximum of one gaseous molecule; (d) there is no interaction between molecules adsorbed in neighboring sites (and therefore, $\overline{E_c} = 0$). Using random distribution of the N molecules in M sites to evaluate $g(N,M)$:

$$g(N, M) = \frac{M!}{N!(M-N)!} \tag{2}$$

The Langmuir isotherm (Langmuir 1918) is obtained:

$$PK = \frac{\theta}{(1-\theta)} \tag{3}$$

where K (the equilibrium constant) is defined by:

$$K = q(T) \exp\left(\frac{\mu^{o,g}}{kT}\right) \tag{4}$$

where $\mu^{o,g}$ is the chemical potential of the molecule in the gas phase at the reference pressure.

The coverage fraction (θ) is defined by:

$$\theta = \frac{N}{M} = \frac{W}{W^*} \tag{5}$$

where W^* is the maximum adsorption capacity of the solid and W is the adsorbed amount.

Fowler and Guggenheim (1939) used the Bragg-William approximation, based on the pairwise additivity and random distribution of neighboring sites, to calculate $\bar{E}_c$:

$$\bar{E}_c = Z \frac{N^2}{2M} u \tag{6}$$

where Z is the coordination number of the lattice and u is the interaction energy parameter. The isotherm expression for pure adsorption is:

$$PK = \frac{\theta}{(1-\theta)} \exp\left(-\theta \frac{u^*}{RT}\right) \tag{7}$$

where K and θ are defined as for the Langmuir isotherm (Eqs. 4 and 5, respectively). The parameter related to the adsorbate–adsorbate interaction energy is:

$$\frac{u^*}{RT} = Z \frac{u}{kT} \tag{8}$$

This model has been tested by many authors, Roque-Malherbe (2000), Koopal and Avena (2001), Tvardovski et al. (2003), Kowalczyk et al. (2004), Hamdaoui and Naffrechoux (2007) and Durimel et al. (2013) with relative success. However, the predictive performance of Fowler and Guggenheim model is limited to more ideal adsorption mixtures.

Honig and Mueller (1962) presented an adaptation of the lattice vacancy theory to pure gas adsorption phenomena. The model uses the Flory–Huggins polymer-monomer solution theory. They consider the polymer (r-mer) analogous to an adsorbed molecule and the monomer analogous to a hole (vacancy). The final expression of this model is:

$$PK = \frac{\theta}{(1-\theta)^r} \exp\left(Z\theta \frac{u}{kT}\right) \tag{9}$$

where K is given by:

$$K = q(T) \exp\left(\frac{\mu^{o,g}}{kT}\right) \exp(r-1) \tag{10}$$

and the coverage fraction θ is defined by:

$$\theta = \frac{rN}{M} = \frac{rW}{W^*} \tag{11}$$

Honig and Mueller (1962) studied the effects of lateral interaction (u/k) and the number of segments (r, directly related to the molecule size). They showed that the shape of the isotherm is strongly affected by these two parameters. The model is able to describe condensation when the lateral interaction parameter (u/k) is attractive.

Nitta et al. (1984) proposed a multi-site occupancy model (MSOM) for homogeneous surfaces, which is essentially the same expression by Honig and Mueller (1962). However, they extended the model to multicomponent adsorption. The extension is:

$$y_i P K_i r_i = \frac{\theta_i}{\left(1 - \sum_{k=1}^{Nc} \theta_k\right)^{r_1}} \exp\left(-r_i \sum_{k=1}^{Nc} \theta_k \frac{u_{ik}}{kT}\right) \tag{12}$$

This model was used by Dunne and Myers (1994), Malek and Farooq (1996), Buss and Heuchel (1997), Mohr

et al. (1999), Grande et al. (2003), Cavenati et al. (2004), Lísal et al. (2008) and Ribeiro et al. (2008) to describe adsorption mixtures with good performances. However, this model is not adequate to predict azeotropelike behavior using only pure component adsorption data. From now on, the multi-site occupancy model proposed by Nitta et al. (1984) will be called MSOM in this work.

Suwanayuen and Danner (1980a, b) developed the vacancy solution model (VSM), based on the vacancy theory, to be applied to adsorption phenomena. The adsorbed phase is treated as a vacancy solution, where the vacancy is an imaginary solvent. Using the criteria of equal chemical potentials of the species presented in different phases, the isotherm is given by:

$$y_i \hat{\varphi}_i P = x_i^s \gamma_i^s \exp\left(\frac{\Delta G_i^o}{RT}\right) \exp\left(\frac{\pi \bar{a}_i}{RT}\right) \quad (13)$$

For each component, Eq. (13) correlates the molar fraction in the gas phase (y_i) with the molar fraction in the adsorbed phase (x_i^s), which is based on the total amount adsorbed, including the vacancy component. In this equation, ΔG_i^o is the standard state free energy of adsorption of the pure i; is the spreading pressure; $\bar{a}_i$ is the partial molar surface area of the i molecule and $\hat{\phi}_i$ is the fugacity coefficient of the i molecule in the gas phase.

The experimental adsorbed molar fraction (x_i) can be correlated with x_i^s as follows:

$$n_m^{s,\infty} = \sum_{i=1}^{Nc} n_i^s + n_v^s = \sum_{i=1}^{Nc} x_i n_i^{s,\infty} \quad (14)$$

$$n_m^s = \sum_{i=1}^{Nc} n_i^s \quad (15)$$

$$x_i^s = \frac{n_i^s}{n_m^{s,\infty}} = \frac{x_i n_m^s}{n_m^{s,\infty}} = x_i \theta \quad (16)$$

$$x_v^s = 1 - \sum_{i=1}^{Nc} x_i^s \quad (17)$$

where $n_m^{s,\infty}$ is the maximum total number of moles of the mixture in the adsorbed phase; n_i^s and n_v^s are the numbers of i molecules and imaginary solvent adsorbed in the mixture, respectively; $n_i^{s,\infty}$ is the maximum total number of moles of each species i in adsorbed phase (for the pure component condition); n_m^s is the total number of moles of the mixture in the adsorbed phase. It is important to notice that the superscript "s" indicates that the variable includes the vacancy species. In Eq. (17), x_v^s is the adsorbed molar fraction of the imaginary solvent (vacancy) in the mixture.

Suwanayuen and Danner (1980b) used the expressions proposed by Lucassen-Reynders (1972, 1973, 1976) to

calculate the product between the spreading pressure and the partial molar areas as:

$$-\frac{\pi \bar{a}_i}{RT} = \left[1 + \frac{n_m^{s,\infty} - n_i^{s,\infty}}{n_m^s}\right] \ln\left(\gamma_v^s x_v^s\right) \quad (18)$$

and the standard state free energy of adsorption as:

$$\exp\left(\frac{\Delta G_i^o}{RT}\right) = \frac{1}{K_i} n_i^{s,\infty} \lim_{x_i^s \to 0} \left(\frac{1}{\gamma_i^s}\right) \quad (19)$$

where K_i, as in the other isotherms, is the adsorption constant related to the intermolecular force between adsorbent and adsorbate.

Suwanayuen and Danner (1980a, b) and many other authors (Hyun and Danner 1982; Talu and Zwiebel 1986; Yu and Neretnieks 1990; Jeong et al. 2007; Heymans et al. 2011; Mofarahi and Gholipour 2014) have tested the VSM using the Margules and Wilson equations to evaluate the activity coefficients of the species in the adsorbed phase: γ_v^s and γ_i^s. Munakata (2007) and Haghtalab and Farzad (2010) used the Non-Random Two-Liquid (NRTL) equation to evaluate these activity coefficients. Reported results show that the VSM model can describe highly non-ideal adsorption behavior.

Applying these equations (Wilson and NRTL) to evaluate the activity coefficient for all Nc species, plus the vacancy present in the adsorbed phase, it is necessary to add an extra component: the vacancy. Therefore, in Eq. (20) the index ($Nc + 1$) indentifies the vacancy, called v. A general expression for the Wilson and NRTL equations is give by:

$$\ln \gamma_i = s\left(1 - \ln \sum_{j=1}^{Nc+1} x_j G_{ji} - \sum_{j=1}^{Nc+1} \frac{x_j G_{ij}}{\sum_{k=1}^{Nc+1} G_{kj} x_k}\right)$$
$$+ p\left[\frac{\sum_{j=1}^{Nc+1} \tau_{ji} G_{ji} x_j}{\sum_{k=1}^{Nc+1} G_{ki} x_k} + \sum_{j=1}^{Nc+1} \frac{x_j G_{ij}}{\sum_{k=1}^{Nc+1} G_{kj} x_k}\left(\tau_{ij} - \frac{\sum_{l=1}^{Nc+1} \tau_{lj} G_{lj} x_l}{\sum_{k=1}^{Nc+1} G_{kj} x_k}\right)\right] \quad (20)$$

where: for Wilsońs equation: $s = 1$; $p = 0$ and $G_{ij} = \Lambda_{ij}$. For the NRTL equation $s = 0$; $p = 1$ and G_{ij} is given by:

$$G_{ij} = \exp\left(-\alpha_{ij} \tau_{ij}\right) \quad (21)$$

where α_{ij} is the nonrandomness parameter for the mixture with components i and j. Also, $\alpha_{ij} = \alpha_{ji}$.

In this work, we used the VSM model with both the Wilson and NRTL equations to evaluate γ_v^s and γ_i^s In both cases, the residual interaction between two adsorbed real molecules (i and $j \neq v$) were neglected. It means that, when using the Wilson equation, the parameters related to those interactions ($\Lambda_{ij} = \Lambda_{ji}$) are equal to 1. Therefore, the

VSM together with the Wilson equation (called here VSM-W) has 4 parameters to be estimated from the pure component adsorption experimental data: K_i, $n_i^{s,\infty}$, Λ_{iv} and Λ_{vi}. In the same way, when the NRTL equation is used to evaluate γ_v^s and γ_i^s, the parameters related to the residual interaction between the two adsorbed real molecules (τ_{ij}, and τ_{ji}) are equal to 1. Then, the VSM with NRTL equation (VSM-N) has 5 parameters: K_i, $n_i^{s,\infty}$, τ_{iv}, τ_{vi}. and α_{iv}. It is important to notice that the solid field contributions to the adsorption phenomena are present not only by the equilibrium constant (K_i), but also, even thought indirectly, by the parameters that take into account the residual interactions between one real molecules (i) and the vacancy (v).

2.1 The proposed Multi-Site Occupancy Model (MSOM-M)

Aiming to improve the performance of existing models, by better taking into account the contributions of molecular size and shape to multicomponent adsorption phenomena, we present a new version of the multi-site occupancy model. The proposed model follows the main idea of the original one (Nitta et al. 1984). Each molecule can occupy multi-sites on a homogeneous surface. However, we propose another expression to account for the number of configurational states and, consequently, a new term for the configurational energy. The detailed step-by-step of development of the expressions is available in supplementary material.

The Guggenheim approximation is used to evaluate the number of configurational states:

$$g(N,M) = \xi^N \frac{M!}{N!(M-rN)!} \left[\frac{(\bar{b}N + M - rN)!}{M!} \right]^{Z/2} \quad (22)$$

the parameter $\bar{b}$ is related to the number of contact pairs per molecule $Z\bar{b}$ (Okada and Nose 1981), which is given by:

$$Z\bar{b} = r(Z-2) + 2 \quad (23)$$

Equation (23) is valid for non-cyclic linear-like molecules, where Z is the coordination number.

The average configurational energy is expressed by:

$$\bar{E}_c = \bar{N}_{11} u \quad (24)$$

Where $\bar{N}_{11}$ is the number of pairs of occupied neighboring sites and u is the interaction energy between an adsorbed pair of molecules. The number of pairs of occupied neighboring sites, considering Bragg-Williams approximation (Hill 1962), is:

$$\bar{N}_{11} = \frac{Z\bar{b}}{r} rN \frac{rN}{2M} \quad (25)$$

Because r is the number of sites occupied by each molecule, we can say that each molecule have r segments

and each segment occupies one site on the homogeneous surface. Therefore, in Eq. (25), $\frac{Z\bar{b}}{r}$ is the number of contact pairs of one segment; rN is the total number of segments adsorbed and $\frac{rN}{2M}$ is the probability of finding a pair of adsorbed segments on the surface. Then, the expression for the average configurational energy is:

$$\bar{E}_c = Z\bar{b} \frac{rN^2 u}{2M} \quad (26)$$

The chemical potential for the adsorbed phase is:

$$\frac{\mu^{ads}}{kT} = -\ln[q(T)\xi] - Z\bar{a} \frac{rN}{M} \frac{u}{kT} - r\ln\left(1 - \frac{rN}{M}\right) + (r-1)\ln\left[1 - 2\frac{(1-r)N}{ZM}\right] + \ln\left(\frac{rN}{M}\right) - \ln r \quad (27)$$

The chemical potential of the molecule in the gas phase can be expressed by:

$$\mu^g = \mu^{o,g} + kT \ln \phi P \quad (28)$$

where ϕ is the fugacity coefficient of the molecule in the gas phase.

Therefore, using the criterion of equal chemical potential in both phases, and rearranging the terms, the pure isotherm of the proposed model is written:

$$P\phi Kr = \frac{\theta(1 - \beta\theta)^{(r-1)}}{(1-\theta)^r} \exp\left(-\bar{b}\theta \frac{u^*}{RT}\right) \quad (29)$$

where:

$$\beta = 2\frac{(r-1)}{Zr} \quad (30)$$

$$K = q(T)\xi \exp\left(\frac{\mu^{o,g}}{kT}\right) \quad (31)$$

and the coverage fraction (θ) is expressed by Eq. (11). The extension for multicomponent adsorption is straight forward. The detailed development of the expressions is available in supplementary material. The Guggenheim approximation for mixtures is:

$$g(\underline{N},M) = \left(\prod_{i=1}^{Nc} \xi_i^{N_i} \right) \frac{M!}{\left(M - \sum_i r_i N_i\right)! \prod_{i=1}^{Nc} (N_i!)} \times \left\{ \frac{\left(\sum_i \bar{b}_i N_i + M - \sum_i r_i N_i\right)!}{M!} \right\}^{\frac{Z}{2}} \quad (32)$$

and the average configurational energy is:

$$\bar{E}_c = \frac{1}{2} \sum_{i=1}^{Nc} \sum_{j=1}^{Nc} Z \frac{\bar{b}_i r_j N_i N_j u_{ij}}{M} \quad (33)$$

Therefore, the expression for the multicomponent adsorption isotherm is:

$$y_i \hat{\phi}_i P K_i r_i = \frac{\theta_i \left(1 - \sum_{k=1}^{Nc} \beta_k \theta_k\right)^{(r-1)}}{\left(1 - \sum_{k=1}^{Nc} \theta_k\right)^{r_i}} \exp\left(-\frac{\bar{b}_i}{2} \sum_{k=1}^{Nc} \theta_k \frac{u_{ik}^*}{RT}\right)$$
$$\times \exp\left(-\frac{r_i}{2} \sum_{k=1}^{Nc} \frac{\bar{b}_k}{r_k} \theta_k \frac{u_{ki}^*}{RT}\right) \quad (34)$$

where θ_i is the coverage fraction of each component i, is given by

$$\theta_i = \frac{r_i N_i}{M} = \frac{r_i W_i}{W*} \quad (35)$$

where r_i is the number of sites occupied by the molecule i and W_i is the adsorbed amount of each component i. K_i is the adsorption constant of each component i (parameter related to the interaction between the solid and the i molecule) and u_{ik} is the parameter related to the intermolecular interaction between molecules i and k adsorbed in neighboring sites.

It is important to observe that the proposed modified MSOM becomes identical to the original model when r is equal to 1. In this case, both models become identical to the Fowler–Guggenheim model. These models becomes the Langmuir isotherm for $r = 1$ and $u_{ij}^* = 0$.

Both ulti-site occupancy models (MSOM and MSOM-M) have four parameters of pure components: W^*, r_i, K_i and u_{ii}^*. However, here, we proposed a procedure to reduce the number of parameters. For the smallest substance, the maximum capacity (W^*) was estimated by regression of the experimental data, using the number of segments r fixed a priori equal to 1. For the other substances, the parameters r_i, K_i and u_{ii}^* were obtained by regression of each experimental data, fixing the maximum capacity of the solid (W^*) as the one obtained previously from the smallest substance. This estimation procedure improves the quality of the parameters (better physical meaning) and decreases the correlation between parameters.

In order to calculate mixtures without any extra parameters, we need a mixing rule to evaluate the cross interaction parameter between a pair of adsorbed molecules in the mixture. The classical mixing rule is the geometric expression:

$$u_{ij}^* = \sqrt{u_{ii}^* u_{jj}^*} \quad (36)$$

However, this classical expression is not really convenient for adsorption, because it cannot be applied to systems containing attraction (positive values) and repulsion (negative values) in the same mixture. In order to improve the combination rule, also including the relative size effect, the cross interaction parameters were calculated using:

Table 1 Mixtures, solids and references of the experimental data of the tested systems

Mixture	Solid	Reference
	13X	Hyun and Danner 1982
C_4H_{10}–C_2H_4		
C_2H_4–CO_2		
C_4H_{10}–C_2H_6		
	H-mordenite	Talu and Ziebel 1986
CO_2–H_2S		
C_3H_8–CO_2		
C_3H_8–H_2S		
CO_2–H_2S–C_3H_8		
	BPL carbon	Yu and Neretnieks 1990
C_7H_{14}–C_7H_8		
C_7H_8–$C_6H_{12}O$		
C_7H_{14}–$C_6H_{12}O$		
C_7H_{14}–C_7H_8–$C_6H_{12}O$		
	DAY13	Sakuth et al. 1998
C_7H_8–C_3H_8O		
	DAY55	Sakuth et al. 1998
C_7H_8–C_3H_8O		
	DAY100	Sakuth et al. 1998
C_7H_8–C_3H_8O		
	ZSM-5	Calleja et al. 1998
CO_2–C_2H_4	(Si/Al = 15)	
CO_2–C_3H_8		
C_2H_4–C_3H_8		
CO_2–C_2H_4–C_3H_8		

$$u_{ij}^* = \frac{\frac{r_i}{r_j} u_{ii}^* + \frac{r_j}{r_i} u_{jj}^*}{r_i + r_j} \quad (37)$$

It is important to notice that for $r_i = r_j = 1$ this rule becomes the classical arithmetic average. Two different coordination numbers ($Z = 4$ and $Z = 5$) were tested for the proposed model.

3 Methodology

In order to evaluate the performance of the models in terms of their ability to predict mixtures using only pure adsorption experimental data, we selected several binary and ternary adsorption mixtures in the literature that present highly non-ideal behaviors. Table 1 presents those mixtures, including the corresponding solids and references.

The parameters were estimated for all models using the software Statistica® 7 to minimize the objective function using pure component adsorption data. We used the mean square of the weighed relative pressure deviation as the objective function:

Table 2 Parameters estimated for MSOM by fitting the experimental data of the pure components

Adsorbate	r_i [–]	K_i [10^3 Pa^{-1}]	u_{ii}/k [K]	DMR (%)
H-mordenite–$W^* = 29.93$ mmol/g				
C_3H_8	12.33	0.058	140.3	14.8
CO_2	1	0.021	−14032.7	14.4
H_2S	3.84	0.441	−1015.2	4.2
13X −T = 298 K–$W^* = 6.23$ mmol/g				
C_2H_4	1.79	0.294	−238.4	10.6
i-C_4H_{10}	2.86	14.568	−368.2	23.3
C_2H_6	2.06	0.013	291.3	4.6
CO_2	1	0.378	−1453.7	13.5
13X −T = 323 K–$W^* = 6.28$ mmol/g				
C_2H_4	1.80	0.070	−177.3	7.7
iC_4H_{10}	3.42	0.723	178.4	14.8
C_2H_6	2.04	0.005	274.7	2.9
CO_2	1	0.093	−1349.3	5.7
BPL Carbon–$W^* = 49.10$ mmol/g				
C_7H_8	1.01	21.69	−20993.0	39.3
$C_6H_{12}O$	1	17.69	−18568.6	20.8
C_7H_{14}	2.02	16.94	−7998.0	26.7
Y-zeolite DAY 13–$W^* = 2.76$ mmol/g				
C_7H_8	1.38	30.554	−176.4	11.2
C_3H_8O	1	15.429	−414.3	4.1
Y-zeolite DAY 55–$W^* = 2.85$ mmol/g				
C_7H_8	1.49	23.481	−103.2	8.0
C_3H_8O	1	1.191	498.6	7.2
Y-zeolite DAY 100–$W^* = 2.88$ mmol/g				
C_7H_8	1.50	15.691	154.4	23.4
C_3H_8O	1	1.600	356.0	5.8
ZSM-5 (Si/Al = 15)–$W^* = 3.94$ mmol/g				
CO_2	1	3.155	−3073.5	12.5
C_2H_4	1.05	15.421	−3890.5	27.6
C_3H_8	2.24	18.392	−312.6	16.2

Table 3 Parameters of the MSOM-M ($Z = 4$) fitted from experimental data of the pure components

Adsorbate	r_i [–]	K_i [10^3 Pa^{-1}]	u_{ii}^*/R [K]	DMR (%)
H-mordenite–$W^* = 29.93$ mmol/g				
C_3H_8	12.65	0.060	20.5	15.1
CO_2	1	0.021	−14032.7	14.4
H_2S	1.51	0.487	−10523.2	3.9
13X −T = 298 K–$W^* = 6.23$ mmol/g				
C_2H_4	1.80	0.298	−377.9	10.6
i-C_4H_{10}	2.86	15.151	−657.1	23.3
C_2H_6	2.07	0.013	336.8	4.5
CO_2	1	0.378	−1453.7	13.5
13X −T = 323 K–$W^* = 6.28$ mmol/g				
C_2H_4.	1.80	0.070	−267.7	7.7
iC_4H_{10}.	3.43	0.770	120.0	15.0
C_2H_6	2.04	0.005	311.2	2.8
CO_2	1	0.093	−1349.3	5.7
BPL Carbon–$W^* = 49.10$ mmol/g				
C_7H_8	1.02	21.69	−20586.0	39.3
$C_6H_{12}O$	1	17.69	−18568.6	20.8
C_7H_{14}	1.77	16.96	−13370.8	26.8
Y-zeolite DAY 13–$W^* = 2.76$ mmol/g				
C_7H_8	1.42	15.284	137.5	19.8
C_3H_8O	1	15.429	−414.3	4.1
Y-zeolite DAY 55–$W^* = 2.85$ mmol/g				
C_7H_8	1.52	18.029	10.7	8.1
C_3H_8O	1	1.191	498.6	7.2
Y-zeolite DAY 100–$W^* = 2.88$ mmol/g				
C_7H_8	1.51	9.860	324.1	22.4
C_3H_8O	1	1.600	356.0	5.8
ZSM-5 (Si/Al = 15)–$W^* = 3.94$ mmol/g				
CO_2	1	3.155	−3073.5	12.5
C_2H_4	1.11	15.015	−3619.8	27.8
C_3H_8	2.24	18.845	−506.7	16.2

$$F_{obj} = \sum_{i=1}^{Np} \left(\frac{P_i^{cal} - P_i^{exp}}{P_i^{exp}} \right)^2 \tag{38}$$

To evaluate the performance of each model the relative mean deviation (RMD) was calculated for the adsorption of each system tested:

$$RMD\ (\%) = \frac{1}{Np} \sum_{i=1}^{Np} \frac{\left| P_i^{cal} - P_i^{exp} \right|}{P_i^{exp}} \times 100\ \% \tag{39}$$

where P_i^{cal} and P_i^{exp} are the pressures obtained by the model and the experimental values, respectively, in each experimental point and Np is the number of points. In the case of mixtures, the relative mean deviation (RMD) was calculated for two types of variables (VAR): the total adsorbed amount and the adsorbed molar fraction. The general expression is analogous to those presented in Eq. (39):

$$RMD\ (\%) = \frac{1}{Np} \sum_{i=1}^{Np} \frac{\left| VAR_i^{cal} - VAR_i^{exp} \right|}{VAR_i^{exp}} \times 100\ \% \tag{40}$$

where VAR can be either the total adsorbed amount or the adsorbed molar fraction. The superscripts *cal* and *exp* indicate the calculated and experimental values, respectively.

4 Results

4.1 Pure correlation

The parameters for all models were estimated by fitting the experimental data from single component adsorption.

Table 4 Parameters of the MSOM-M ($Z = 4$) fitted from experimental data of the pure components

Adsorbate	r_i [–]	K_i [10^3 Pa^{-1}]	u_{ii}^*/R [K]	DMR (%)
H-mordenite–$W^* = 29.93$ mmol/g				
C$_3$H$_8$	12.53	0.059	59.5	15.0
CO$_2$	1	0.021	−14032.7	14.4
H$_2$S	1.55	0.487	−9673.9	3.9
13X –T = 298 K–$W^* = 6.23$ mmol/g				
C$_2$H$_4$	1.79	0.299	−354.1	10.6
i-C$_4$H$_{10}$	2.86	14.918	−575.9	23.3
C$_2$H$_6$	2.07	0.013	325.7	4.5
CO$_2$	1	0.378	−1453.7	13.5
13X –T = 323 K–$W^* = 6.28$ mmol/g				
C$_2$H$_4$	1.80	0.070	−245.9	7.7
iC$_4$H$_{10}$	3.43	0.750	141.7	14.9
C$_2$H$_6$	2.00	0.005	277.2	3.0
CO$_2$	1	0.093	−1349.3	5.7
BPL Carbon–$W^* = 49.10$ mmol/g				
C$_7$H$_8$	1.10	21.7	−18122.5	39.3
C$_6$H$_{12}$O	1	17.7	−18568.6	20.8
C$_7$H$_{14}$	1.82	17.0	−12108.6	26.7
DAY 13–$W^* = 2.76$ mmol/g				
C$_7$H$_8$	1.42	15.388	134.4	19.8
C$_3$H$_8$O	1	15.429	−414.3	4.1
DAY 55–$W^* = 2.85$ mmol/g				
C$_7$H$_8$	1.51	18.063	14.5	11.4
C$_3$H$_8$O	1	1.191	498.6	7.2
DAY 100–$W^* = 2.88$ mmol/g				
C$_7$H$_8$	1.51	8.940	371.2	22.3
C$_3$H$_8$O	1	1.600	356.0	5.8
ZSM-5 (Si/Al = 15) –$W^* = 3.94$ mmol/g				
CO$_2$	1	3.155	−3073.5	12.5
C$_2$H$_4$	1.11	14.939	−3599.8	27.8
C$_3$H$_8$	2.24	18.578	−453.0	16.2

Table 5 Parameters estimated for VSM-W by fitting the experimental data of the pure components

Adsorbate	K_i [10^3 Pa^{-1}]	$N_i^{s,\infty}$ [mmol/g]	Λ_{1v}	Λ_{v1}	RMD (%)
H-mordenite					
C$_3$H$_8$	2.100	1.61	7.22	2.13	18.3
CO$_2$	2.101	3.22	0.18	5.52	3.2
H$_2$S	8.817	3.36	5.28	2.23	8.4
13X –T = 298 K					
C$_2$H$_4$	1.161	2.97	0.45	3.30	7.4
i-C$_4$H$_{10}$	28.990	2.19	8.40	2.30	24.8
C$_2$H$_6$	0.082	2.54	1.09	0.53	3.3
CO$_2$	6.383	4.44	0.21	4.88	6.8
13X –T = 323 K					
C$_2$H$_4$	0.182	2.83	0.62	2.21	6.3
i-C$_4$H$_{10}$	2.609	1.95	16.31	0.40	14.2
C$_2$H$_6$	0.034	2.29	1.24	0.34	2.1
CO$_2$	0.075	4.21	0.04	4.62	3.7
BPL Carbon					
C$_7$H$_8$	4,301.9	11.01	0.13	8.91	7.8
C$_6$H$_{12}$O	3,620.0	51.57	0.16	13.24	11.0
C$_7$H$_{14}$	3,961.3	34.13	0.06	15.71	3.9
DAY 13					
C$_7$H$_8$	78.920	2.08	5.41	0.18	10.6
C$_3$H$_8$O	16.345	2.71	0.02	4.33	5.3
DAY 55					
C$_7$H$_8$	77.322	1.90	2.64	0.80	8.2
C$_3$H$_8$O	3.553	2.80	0.80	0.45	6.5
DAY 100					
C$_7$H$_8$	31.894	1.89	0.12	2.80	26.2
C$_3$H$_8$O	4.876	2.82	1.03	0.42	4.9
ZSM 5 (Si/Al = 15)					
CO$_2$	10.057	2.96	5.23	3.04	17.4
C$_2$H$_4$	18.062	2.49	7.85	2.35	48.4
C$_3$H$_8$	25.023	1.88	11.00	0.79	15.7

Tables 2, 3 and 4 present the estimated parameters and the relative mean deviation (RMD) for the multi-site occupancy models tested: MSOM, MSOM-M ($Z = 4$) and MSOM ($Z = 5$), respectively.

Tables 5 and 6 present the estimated parameters and the relative mean deviation (RMD) for the VSM models using Wilson and NRTL equations (VSM-W and VSM-N), respectively

Figure 1 shows a typical result found in the correlation of the pure adsorption data by the models MSOM, MSOM-M, VSM-W and VSM-N. It can be observed that the models are able to represent, to a good extent, the pure component experimental isotherm.

In Tables 2, 3 and 4 we can observe that the parameters for all the multi-site occupancy models are very similar. As

expected, the major difference is observed in the adsorbate–adsorbate interaction (u^*/R).

The majority of the experimental adsorption data used to evaluate the parameters were obtained under low pressure, and therefore, present small coverage fraction. In this region the adsorbate–absorbate interaction does not play an important rule. Then, in order to observe how this parameter affects the performance of the multi-site occupancy models (MSOM and MSOM-M), some runs were made at pressures higher than those of the experimental data. Figure 2 presents these runs for the adsorption of H$_2$S in H-mordenite at 303.15 K and C$_2$H$_4$, in 13X at 323.15 K. The effect of adsorbate–adsorbate interaction could be observed, especially for the case of the H$_2$S adsorption.

Table 6 Parameters estimated for VSM-N by fitting the experimental data of the pure components

Adsorbate H-mordenite	K_i [10^3 Pa^{-1}]	$N_i^{s,\infty}$ [mmol/g]	Λ_{iv}	Λ_{vi}	α_{iv}	RMD (%)
C_3H_8	1.540	2.17	0.37	−5.63	0.10	14.0
CO_2	1.006	3.87	−1.97	1.85	0.35	5.1
H_2S	20.357	4.54	−1.80	−1.77	0.29	3.9
13X T = 323 K						
C_2H_4	2.626	2.97	−1.03	0.47	0.47	7.7
i-C_4H_{10}	7.530	2.98	3.60	−8.86	0.08	22.0
C_2H_6	0.083	2.54	1.06	−0.47	0.22	3.3
CO_2	4.056	4.32	−1.22	1.18	0.64	7.4
13X T = 323 K						
C_2H_4	0.469	2.79	−1.11	1.54	0.52	6.2
i-C_4H_{10}	3.345	2.52	−2.32	−7.23	0.23	12.0
C_2H_6	0.035	2.32	1.28	−0.49	0.29	2.1
CO_2	0.686	4.06	−1.03	0.97	0.58	4.3
BPL Carbon						
C_7H_8	5,290.7	4.85	−1.57	0.94	0.65	11.6
$C_6H_{12}O$	3,504.3	5.49	−2.22	0.45	0.42	4.9
C_7H_{14}	4,314.0	2.97	−3.00	2.85	0.24	3.4
DAY 13						
C_7H_8	30.429	2.80	−1.10	−4.05	0.40	11.2
C_3H_8O	29.026	2.90	0.45	−0.91	0.63	3.7
DAY 55						
C_7H_8	3.373	1.83	−1.00	4.92	0.62	7.2
C_3H_8O	3.123	2.87	0.02	0.83	0.23	7.8
DAY 100						
C_7H_8	0.668	1.89	−0.76	5.06	0.38	25.0
C_3H_8O	4.944	2.82	1.59	−0.69	0.17	4.7
ZSM-5 (Si/Al = 15)						
CO_2	39.053	4.15	−2.31	−1.71	0.30	8.4
C_2H_4	2.776	1.99	9.60	−2.96	0.25	23.3
C_3H_8	65.116	1.71	−0.56	−1.38	0.42	17.1

It is important to pointed out that, because of the number of parameters (5) of the VSM-N, the optimization procedure presented several minima. It means that more than one set of parameters are statistically equivalent. Therefore, the set of parameters presented in Table 6 was chosen by imposing extra restrictions. By definition, when α_{ij} is zero, the mixture is completely random (Renon and Prausnitz 1968) and negative numbers are meaningless. Also, according to Prausnitz et al. (1999) a typical choice is $\alpha_{ij} = 0.3$. Therefore, we selected the set of parameters with the smallest but positive value of the randomness parameter (α_{iv}).

4.2 Mixture prediction

Using only the parameters obtained from the pure adsorption experimental data, we show the performance of

5 models (MSOM; MSOM-M ($Z = 4$); MSOM-M ($Z = 5$); VSM-W, and VSM-N) in terms of predictive calculations of binary and ternary adsorption mixtures.
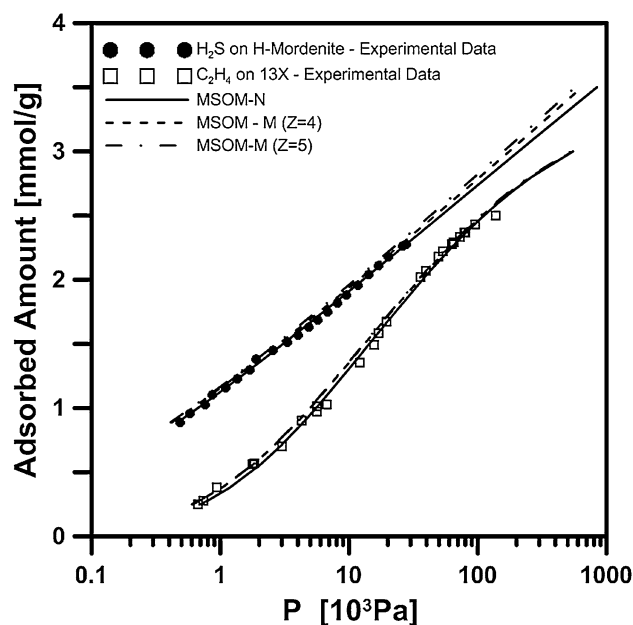
To illustrate the results, we selected one binary mixture from each solid to present the typical phase diagram. Figure 3 presents the results obtained for the system of C_3H_8-H_2S in H-mordenite at 303 K at P = 8.14 × 10^3 Pa. This mixture presents a highly non-ideal behavior, including an inversion of selectivity (azeotropelike behavior). Among all models studied, just the MSOM-M proposed here, using both coordination numbers ($Z = 4$ and $Z = 5$), were able to predict this behavior.

Figure 3 shows that the MSOM-M models presented similar performance with both coordination numbers ($Z = 4$ and $Z = 5$). This equivalent performance was observed for this and other mixtures in the same solid. However, all these systems are at low pressure, condition
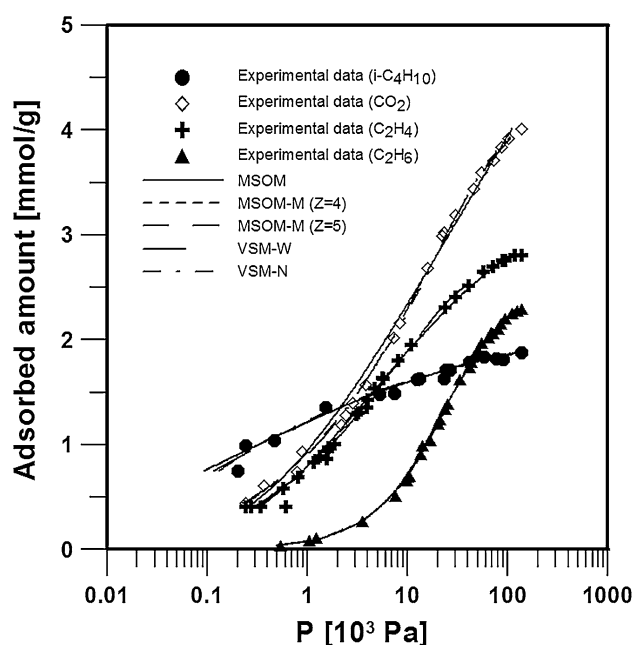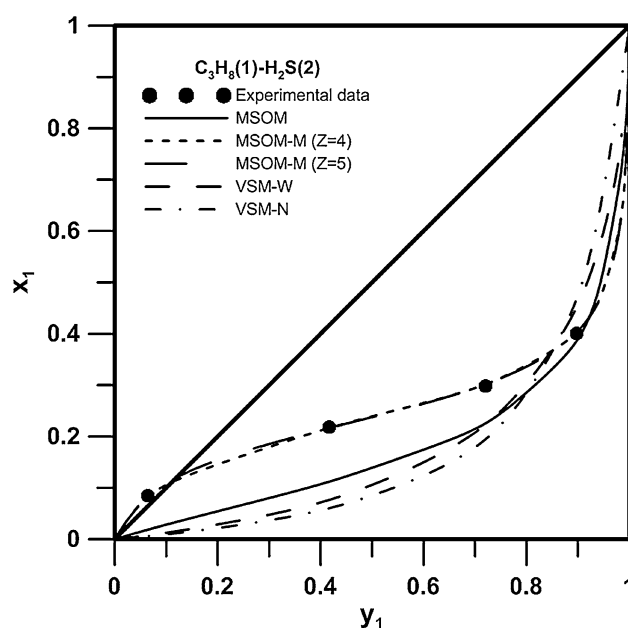
Fig. 1 Pure gas adsorption isotherms (i–C_4H_{10}, C_2H_4, CO_2 and C_2H_6) on 13X zeolite at 298 K. Experimental data are of Hyun and Danner (1982)

Fig. 3 Phase diagram for adsorption of C_3H_8–H_2S on H-mordenite at 303 K and P = 8.14×10^3 Pa. Models and experimental data (Talu and Zwiebel 1986)
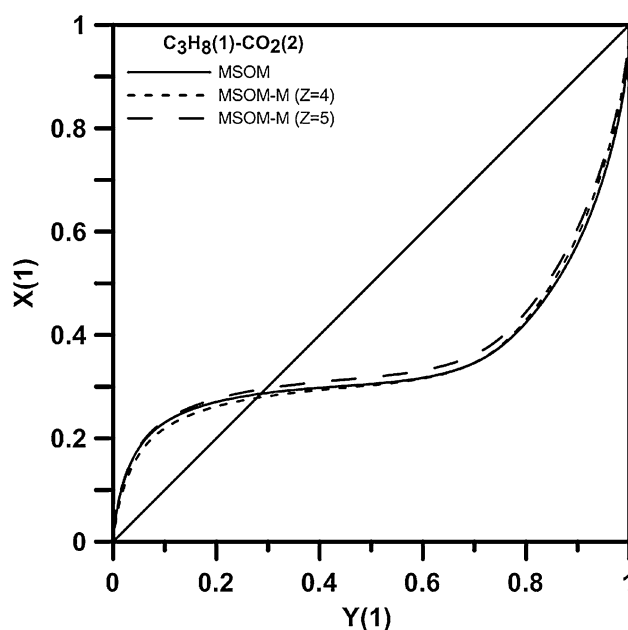

Fig. 2 Adsorption isotherms of pure components (C_2H_4 on 13X zeolite at 323 K—exp. data of Hyun and Danner 1982 and H_2S on H-mordenite at 303 K—exp. data of Talu and Zwiebel 1986)

Fig. 4 Phase diagram for adsorption of C_3H_8–CO_2 on H-mordenite at 303 K and P = 3×10^5 Pa

at which the adsorbate–adsorbate interaction parameter has a small contribution. In order to notice the effect of this parameter at a higher pressure, the MSOM-M models were used to predict the adsorption of C_3H_8–CO_2 in H-mordenite at 303 K at P = 3×10^5 Pa. Figure 4 shows

the results for the MSOM-M using $Z = 4$ and $Z = 5$. Even at this condition, they show undistinguishable performance. Therefore, from now on, only results obtained from the MSOM-M with $Z = 4$ are explicitly presented in the figures. Results for all models and mixtures are

Table 7 Deviations (RMD and ARMD) observed in the prediction of all binary mixtures adsorption

Mixture (1)–(2)	RMD [%]									
	MSOM		MSOM-M (Z = 4)		MSOM-M (Z = 5)		VSM-W		VSM-N	
	x_1	W^T	x_1	W^T	x_1	W^T	x_1	W^T	x_1	W^T
H-mordenite T = 303 K										
C_3H_8–CO_2 (P = 4.10×10^4 Pa)	17.0	8.0	13.7	9.9	14.7	9.4	27.0	8.7	24.0	9.4
C_3H_8–H_2S (P = 8.14×10^3 Pa)	38.7	3.9	1.0	15.7	1.1	15.7	48.4	7.6	54.2	7.0
CO_2–H_2S (P = 1.51×10^4 Pa)	107.8	20.3	7.4	4.9	9.5	5.3	18.4	2.0	25.6	1.6
ARMD [%]	54.5	10.7	7.4	10.2	8.4	10.1	31.3	6.1	34.6	6.0
13X T = 298 K										
i-C_4H_{10}–C_2H_4 (P = 1.38×10^5 Pa)	13.1	2.9	13.4	2.9	13.4	3.0	21.6	9.9	67.8	8.4
C_2H_4–CO_2 (P = 1.38×10^5 Pa)	8.1	6.7	7.8	6.4	7.8	6.5	54.3	1.4	24.0	1.6
i–C_4H_{10}–C_2H_6 (P = 1.38×10^5 Pa)	33.2	5.4	33.4	5.1	33.3	5.1	17.0	7.3	27.9	4.6
ARMD [%]	18.1	5.0	18.2	4.8	18.2	4.9	30.9	6.2	39.9	4.9
13X T = 323 K										
i-C_4H_{10}–C_2H_4 (P = 1.38×10^5 Pa)	5.1	3.0	4.3	3.0	4.3	3.0	26.8	11.1	85.8	9.7
C_2H_4–CO_2 (P = 1.38×10^5 Pa)	7.8	6.6	7.4	6.3	7.6	6.4	21.1	23.4	7.6	1.3
i–C_4H_{10}–C_2H_6 (P = 1.38×10^5 Pa)	32.7	7.3	30.3	6.6	29.7	6.4	12.5	8.0	67.0	2.7
ARMD [%]	15.2	5.7	14.0	5.3	13.9	5.3	20.1	14.2	53.4	4.6
BPL Carbon T = 298 K										
C_7H_{14}–C_7H_8 (P = 1.00×10^0 Pa)	11.6	26.1	10.1	22.3	10.2	24.2	9.5	5.8	49.0	5.4
C_7H_8–$C_6H_{12}O$ (P = 1.00×10^0 Pa)	13.0	12.5	12.7	12.8	11.6	14.0	13.8	19.5	58.3	13.3
C_7H_{14}–$C_6H_{12}O$ (P = 1.00×10^0 Pa)	80.4	32.9	58.6	28.5	63.2	29.4	8.5	12.6	424.5	19.0
ARMD [%]	35.0	23.8	27.1	21.2	28.3	22.5	10.6	12.6	177.3	12.6
DAY 13 T = 318 K										
C_7H_8–$C_6H_{12}O$ (P = 3.50×10^2 Pa)	25.6	9.6	22.3	7.1	22.4	7.2	22.5	11.8	50.4	11.6
C_7H_8–$C_6H_{12}O$ (P = 1.05×10^3 Pa)	20.3	4.2	17.8	2.8	17.9	2.9	20.5	7.8	69.9	4.1
ARMD [%]	22.9	6.9	20.1	5.0	20.1	5.0	21.5	9.8	60.1	7.9
DAY 55 T = 318 K										
$C_7H_8 \times C_6H_{12}O$ (P = 3.50×10^2 Pa)	19.0	12.9	17.8	11.8	17.8	11.4	14.6	8.6	20.0	7.3
C_7H_8–$C_6H_{12}O$ (P = 1.05×10^3 Pa)	16.1	6.5	16.2	6.3	16.1	5.8	9.6	1.8	14.0	1.3
ARMD [%]	17.5	9.7	17.0	9.0	16.9	8.6	12.1	5.2	17.0	4.3
DAY100 T = 318 K										
C_7H_8–$C_6H_{12}O$ (P = 3.50×10^2 Pa)	12.6	8.2	8.4	7.1	8.2	6.3	4.6	4.8	4.3	3.3
C_7H_8–$C_6H_{12}O$ (P = 1.05×10^3 Pa)	8.8	4.2	8.9	2.9	8.7	2.7	3.7	1.3	4.7	1.5
ARMD [%]	10.7	6.2	8.6	5.0	8.4	4.5	4.2	3.1	4.5	2.4
ZSM-5 (Si/Al = 15) T = 293 K										
CO_2–C_2H_4 (P = 1.00×10^4 Pa)	4.1	7.0	1.5	7.8	1.4	7.8	2.7	13.4	61.7	16.8
CO_2–C_2H_4 (P = 9.03×10^4 Pa)	4.0	2.6	4.6	1.9	4.6	1.9	6.3	1.8	98.6	1.8
CO_2–C_3H_8 (P = 9.14×10^4 Pa)	28.4	13.8	26.8	13.2	27.5	13.4	14.2	2.8	20.6	16.2
C_2H_4–C_3H_8 (P = 1.01×10^4 Pa)	10.2	15.1	9.5	14.5	9.6	14.6	39.1	7.2	78.3	2.2
C_2H_4–C_3H_8 (P = 8.75×10^4 Pa)	19.0	16.6	17.9	15.4	18.0	15.5	27.9	1.5	79.8	7.4
ARMD [%]	13.1	11.0	12.1	10.6	12.2	10.6	18.0	5.3	67.8	8.9

RMD calculated by Eq. (40), ARMD means average of RMD

presented in terms of their relative mean deviations in Tables 7 and 8, for all tested binary and ternary mixtures, respectively.

Figure 5 presents results for C_7H_8-$C_6H_{12}O$ mixtures adsorbed on carbon at 1 Pa. Although the selectivity is very small, the mixture present an inversion of selectivity. Only

Table 8 Relative mean deviation observed in the prediction of ternaries mixture adsorption

Model		RMD [%][a]			
		CO_2–H_2S–C_3H_8[b]	C_7H_{14}–C_7H_8–$C_6H_{12}O$[c]	CO_2–C_2H_4–C_3H_8[d]	CO_2–C_2H_4–C_3H_8[e]
MSOM	x_1	99.7	65.6	28.4	16.4
	x_2	5.3	15.0	17.3	13.9
	x_3	31.8	17.5	8.5	11.2
	n_t	5.3	26.0	25.7	14.7
MSOM-M (Z = 4)	x_1	8.2	40.3	28.4	15.7
	x_2	1.9	14.5	16.3	13.2
	x_3	1.6	15.4	8.1	10.8
	n_t	5.1	22.9	25.0	13.9
MSOM-M (Z = 5)	x_1	8.9	44.9	29.8	16.2
	x_2	2.2	12.6	16.6	13.4
	x_3	1.5	15.5	8.1	10.8
	n_t	5.4	24.8	25.2	14.1
VSM-W	x_1	52.5	42.9	28.8	14.4
	x_2	9.9	18.2	47.2	42.5
	x_3	21.6	16.8	9.4	18.0
	n_t	26.3	20.0	11.11	1.9

[a] RMD calculated by Eq. (40)

[b] H-mordenite/303 K/1.34×10^4 Pa

[c] BPL/298 K/1 Pa
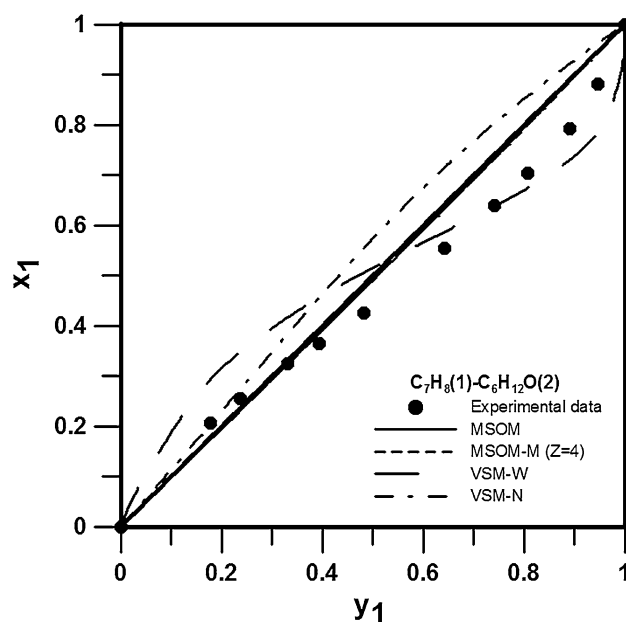
[d] ZSM-5/293 K/3.04×10^4 Pa

[e] ZSM-5/293 K/8.19×10^4 Pa

Fig. 5 Phase diagram for adsorption of C_7H_8–$C_6H_{12}O$ on BPL Carbon at 298 K and P = 1 Pa. Models and experimental data (Yu and Neretnieks 1990)

the VSM-W predicted the azeotropelike behavior shown by this mixture. For this case, none of the multi-site occupancy models, MSOM or MSOM-M, present selectivity. The adsorbed molar fractions predicted by the MSOM and MSOM-M models are about the same as the molar fraction of the gas phase.

Figure 6 presents the predictive calculations of binary mixtures of i-C_4H_{10}-C_2H_4 adsorbed in 13× at 298 K and 1.38×10^5 Pa. Among all the tested models, only the MSOM predicted the azeotropelike behavior.

Figure 7 presents results of predictive calculations of binary mixtures of C_2H_4-C_3H_8 adsorption in ZSM-5 at 293 K. Once again, only the MSOM and MSOM-M models predicted the azeotropelike behavior. However, these models over predicted the total amount adsorbed.

Table 7 gives the results for all binary mixtures tested in this work. It is remarkable to see in this Table that the VSM-N presented the worst performance in predicting mixture behavior for all binary adsorptions studied here. This result is somewhat surprising because this model

presented, in general, the best adjustment for the pure adsorption data. One possible explanation is that the quality of the adjustment is more related to the large number of parameters (5) than to the physical characteristics of the model. We noticed a high degree of parameter correlation for the VSM-N model. In general, the multi-site occupancy models (MSOM and MSOM-M) presented better results, excluding the mixtures adsorbed in BPL Carbon, for which the VSM-W presented the best performance. This could be explained by the low coverage fraction or low pressure (1 Pa) of the experimental data. At this condition, the most important contribution to describe the adsorption behavior is related to the adsorbate-adsorbent interaction. In the MSOM there is only one parameter related directly to this interaction, while in the VSM-W three parameters are related to this interaction: the equilibrium constant (K), Λ_{iv} and Λ_{vi}. Another point to be highlighted is the fact that the adsorption experimental data of the pure components used in the parameter fitting were collected in a very narrow range of low pressure. The lack of data at higher pressures undermined the quality of the majority of the MSOM-M parameters, such as W^* and u_{ii}^*. On the opposite side, just one ($n_i^{s,\infty}$) of the 4 parameters of the VSM-W was undermined by the lack of experimental data at higher pressure.

From all 23 binary mixtures tested here, 13 of them present azeotropelike behavior. The models MSOM, MSOM-M, VSM-W, and VSM-N could predict 8, 10, 6, and 3 of them, respectively.

Among all ternary mixtures studied here, we present graphically the adsorption of CO_2-H_2S-C_3H_8 in
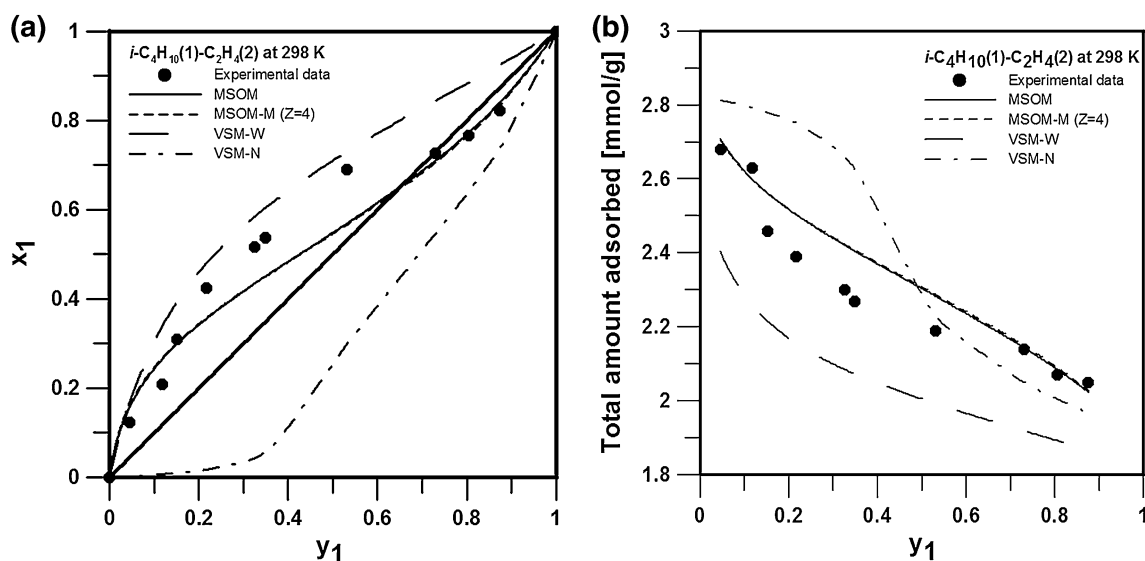
Fig. 6 Phase diagram for adsorption of i–C_4H_{10}–C_2H_4 (**a**)-Adsorbed fraction (**b**)-total adsorbed amount. Values predicted by the models and experimental data (Hyun and Danner 1982)
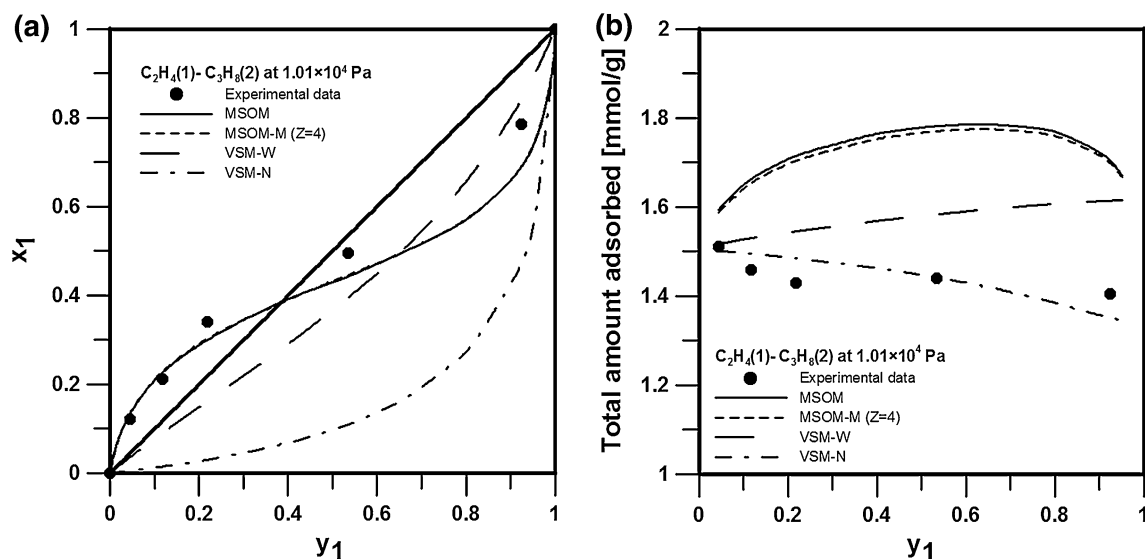

Fig. 7 Adsorption of C_2H_4–C_3H_8 on ZSM-5 at 293 K: **a** adsorbed molar fraction; **b** total amount adsorbed, versus gas molar fraction. Models and experimental data (Calleja et al. 1998)

H-mordenite at 303 K and 1.34×10^4 Pa. This mixture presents azeotropelike behavior (as shown in the Fig. 8.

Table 8 shows the results of predictive calculations of all adsorbed ternary systems that were evaluated is this work. Because calculations using the VSM-N model presented unphysical results, these calculations are not shown in this table. The good performance of the multi-site occupancy models (MSOM and MSOM-M) can be observed. Among the 6 azeotropelike crossover behaviors presented by the ternary mixtures, the MSOM-M proposed

here was able to predict 5 of them, using both coordination numbers ($Z = 4$ and $Z = 5$). The original multi-site occupancy model (MSOM) and VSM-W predicted 1 and 4, respectively.

It can be seen in Fig. 8a, b that the proposed MSOM-M correctly predicted the azeotropelike crossover presented by the molar fraction of propane. Even thought the VSM-W model predicted the selectivity inversion in terms of molar fraction in propane, it describes this behavior in the opposite direction, as shown in Fig. 8b.
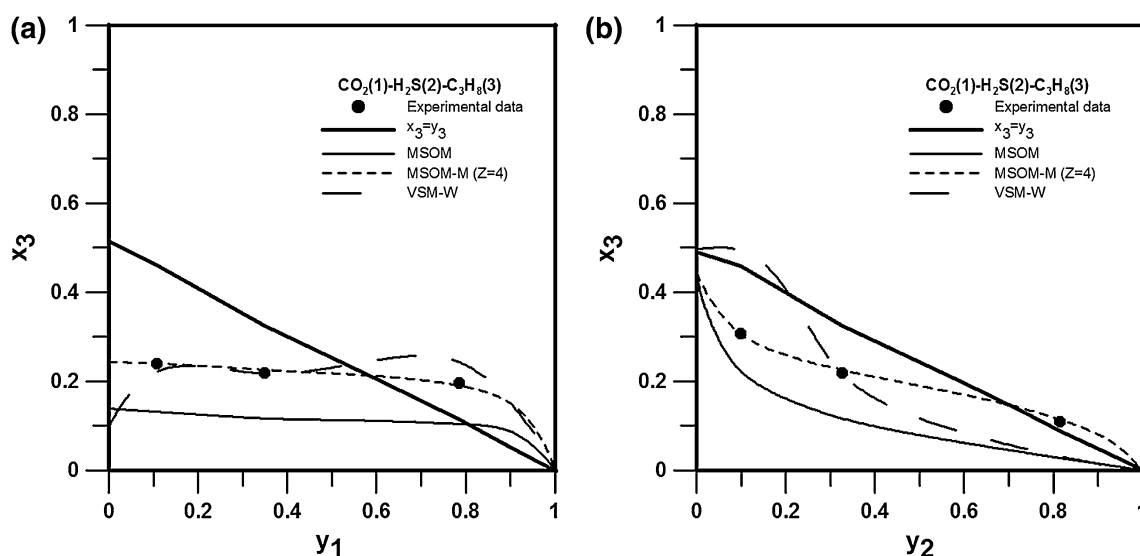
Fig. 8 Adsorbed molar fraction of propane as a function of the increase of gas molar fraction of: (**a**) CO_2–($y_3/y_2 = 1.0621$); (**b**) H_2S–($y_3/y_1 = 0.9635$); on H-mordenite at 303 K and 1.34×10^4 Pa. Experimental data of Talu and Zwiebel (1986)

5 Conclusion

Here, we presented a modified version of the multi-site occupancy model (MSOM-M) proposed originally by Nitta et al. (1984). The performance of the proposed model (MSOM-M) was evaluated in terms the capacity of its predictive description of binary and ternary adsorption mixtures. The model parameters were estimated by fitting the experimental adsorption data of pure substances. The performance of the proposed model was compared to those obtained from the original MSOM and to the vacancy solution model (VSM) presented by Suwanayuen and Danner (1980a, b). In general, the proposed model showed better performance in predicting the binary and ternary mixtures studied, when compared to the Vacancy Solution Models (excluding the mixtures adsorbed in BPL Carbon, for which the VSM-W presented the best performance). This fact suggests that the relative size of the molecules is an important parameter to describe adsorptions, especially for mixtures that present azeotropelike behavior.

The poor performance presented by the multi-site occupancy models in predicting binary and ternary mixtures, on BPL carbon at 1 Pa, can be attributed to the very narrow range of low pressure of the experimental data of the pure components, which undermined the quality of the estimated parameters, and therefore, the mixture prediction.

References

Buss, E., Heuchel, M.: Adsorption equilibria of methane and tetrafluoromethane and their binary mixtures on silicalite. J. Chem. Soc. Faraday Trans. **93**, 1621–1628 (1997)

Calleja, G., Pau, J., Calles, J.A.: Pure and multicomponent adsorption equilibrium of carbon dioxide, ethylene, and propane on ZSM-5 zeolites with different Si/Al ratios. J. Chem. Eng. Data **43**, 994–1003 (1998)

Cavenati, S., Grande, C.A., Rodrigues, A.E.: Adsorption equilibrium of methane, carbon dioxide, and nitrogen on zeolite 13X at high pressures. J. Chem. Eng. Data **49**, 1095–1101 (2004)

Dunne, J., Myers, A.L.: Adsorption of gas mixtures in micropores: effect of difference in size of adsorbate molecules. Chem. Eng. Sci. **49**, 2941–2951 (1994)

Durimel, A., Altenor, S., Miranda-Quintana, R., Du Mesnil, P.C., Jauregui-Haza, U., Gadiou, R., Gaspard, S: pH dependence of chlordecone adsorption on activated carbons and role of adsorbent physico-chemical properties. Chem. Eng. J. **229**, 239–249 (2013)

Fowler, R.H., Guggenheim, E.A.: Statistical Thermodynamics. Cambridge University Press, London (1939)

Grande, C.A., Gigola, C., Rodrigues, A.E.: Propane-propylene binary adsorption on zeolite 4A. Adsorption **9**, 321–329 (2003)

Haghtalab, A., Farzad, S.: A new gas adsorption isotherm using the vacancy solution theory and NRTL activity coefficient model. Fluid Phase Equilib. **292**, 36–41 (2010)

Hamdaoui, O., Naffrechoux, E.: Modeling of adsorption isotherms of phenol and chlorophenols onto granular activated carbon: Part I. Two-parameter models and equations allowing determination of thermodynamic parameters. J. Hazard. Mater. 147, 381–394 (2007)

Heymans, N., Alban, B., Moreau, S., De Weireld, G.: Experimental and theoretical study of the adsorption of pure and binary systems containing methane, carbon monoxide, carbon dioxide and nitrogen. Application to the syngas generation. Chem. Eng. Sci. **66**, 3850–3858 (2011)

Hill, T.L.: An introduction to statistical thermodynamics. Addison-Wesley Publishing Company, London (1962)

Honig, J.M., Mueller, C.R.: Adaptation of lattice vacancy theory to gas adsorption phenomena. J. Phys. Chem. **66**, 1305–1308 (1962)

Hyun, S.H., Danner, R.P.: Equilibrium adsorption of ethane, ethylene, isobutene, carbon dioxide and their mixtures. J. Chem. Eng. Data **27**, 196–200 (1982)

Jeong, B., Ahn, E., Yun, J., Lee, C., Choi, D.: Ternary adsorption equilibrium of $H_2/CH_4/C_2H_4$ onto activated carbon. Sep. Purif. Technol. **55**, 335–342 (2007)

Koopal, L.K., Avena, M.J.: A simple model for adsorption kinetics at charged solid-liquid interfaces. Colloids Surf. A **192**, 93–107 (2001)

Kowalczyk, P., Tanaka, H., Kanoh, H., Kaneko, K.: Adsorption Energy Distribution from the Aranovich-Donohue Lattice Density Functional Theory. Langmuir **20**, 2324–2332 (2004)

Langmuir, I.: Adsorption of gases on glass, mica and platinum. J. Am. Chem. Soc. **40**, 1361–1403 (1918)

Lísal, M., Cosoli, P., Smith, W.R., Jain, S.K., Gubbins, K.E.: Molecular-level simulations of chemical reaction equilibrium for nitric oxide dimerization reaction in disordered nanoporous carbons. Fluid Phase Equilib. **272**, 18–31 (2008)

Lucassen-Reynders, E.H.: A surface equation of state for mixed surfactant monolayers. J. Colloid Interface Sci. **41**, 156–167 (1972)

Lucassen-Reynders, E.H.: Interactions in mixed monolayers I. Assessment of interaction between surfactants. J. Colloid Interface Sci. **42**, 554–562 (1973)

Lucassen-Reynders, E.H.: Adsorption of surfactant monolayers at gas/liquid and liquid/liquid interfaces. Prog Surf. Membr. Sci. **10**, 253–360 (1976)

Malek, A., Farooq, S.: Comparison of isotherm models for hydrocarbon adsorption on activated carbon. AIChE J. **42**, 3191–3201 (1996)

Mofarahi, M., Gholipour, F.: Gas adsorption separation of CO_2/CH_4 system using zeolite 5A. Microporous and mesoporous materials. Microporous Mesoporous Mater. 200, 1–10 (2014)

Mohr, R.J., Vorkapic, D., Rao, M.B., Sircar, S.: Pure and binary gas adsorption equilibria and kinetics of methane and nitrogen on 4A zeolite by isotope exchange technique. Adsorption **5**, 145–158 (1999)

Munakata, K.: Vacancy solution model formulated by the NRTL equation for correlation of adsorption equilibria. J. Chem. Eng. Jpn. **40**, 398–409 (2007)

Nitta, T., Shigetomi, T., Kuro-Oka, M.E., Katayama, T.: An adsorption isotherm of multi-site occupancy model for homogeneous surface. J. Chem. Eng. Jpn. **17**, 39–44 (1984)

Okada, M., Nose, T.: Treatment of the hole theory for r-mers. I. Pure liquids. Polym. J. **13**, 399–406 (1981)

Prausnitz, J.M., Lichtenthaler, R.N., Azevedo, E.G.: Molecular thermodynamics of fluid-phase equilibria. Prentice Hall International Inc, New Jersey (1999)

Renon, H., Prausnitz, J.M.: Local composition in thermodynamic excess functions for liquid mixtures. AIChE J. **14**, 135–144 (1968)

Ribeiro, R.P., Sauer, T.P., Lopes, F.V., Moreira, R.F., Grande, C.A., Rodrigues, A.E.: Adsorption of CO_2, CH_4, and N_2 in activated carbon honeycomb monolith. J. Chem. Eng. Data **53**, 2311–2317 (2008)

Roque-Malherbe, R.: Complementary approach to the volume filling theory of adsorption in zeolites. Microporous and Mesoporous Mater. **41**, 227–240 (2000)

Sakuth, M., Meyer, J., Gmehling, J.: Measurement and prediction of binary adsorption equilibria of vapors on dealuminated Y-zeolites (DAY). Chem. Eng. Process. **37**, 267–277 (1998)

Suwanayuen, S., Danner, R.P.: A gas adsorption isotherm equation based on vacancy solution theory. AIChE J. **26**, 68–76 (1980a)

Suwanayuen, S., Danner, R.P.: Vacancy solution theory of adsorption from gas mixtures. AIChE J. **26**, 76–83 (1980b)

Talu, O., Zwiebel, I.: Multicomponent adsorption equilibria of nonideal mixtures. AIChE J. **32**, 1263–1270 (1986)

Tvardovski, A., Tondeur, D., Favre, E.: Description of multicomponent adsorption and absorption phenomena from a single viewpoint. J. Colloid Interface Sci. **256**, 239–244 (2003)

Yu, J.: Neretnieks. I.: Single component and multicomponent adsorption equilibria on activated carbon of methylcyclohexane, toluene and isobuthyl methyl ketone. Ind. Eng. Chem. Res. **29**, 220–231 (1990)